

PAPER

Frequency-Domain ICI Cancellation with MMSE Equalization for DS-CDMA Downlink

Kazuaki TAKEDA^{†a)}, Koichi ISHIHARA[†], *Student Members*, and Fumiya ADACHI[†], *Member*

SUMMARY Frequency-domain equalization (FDE) based on the minimum mean square error (MMSE) criterion can replace the conventional rake combining while offering significantly improved bit error rate (BER) performance for the downlink DS-CDMA in a frequency-selective fading channel. However, the presence of residual inter-chip-interference (ICI) after FDE produces orthogonality distortion among the spreading codes and the BER performance degrades as the level of multiplexing increases. In this paper, we propose a joint MMSE frequency-domain equalization (FDE) and ICI cancellation to improve the BER performance of the DS-CDMA downlink. In the proposed scheme, the residual ICI replica in the frequency-domain is generated and subtracted from each frequency component of the received signal after MMSE-FDE. The MMSE weight at each iteration is derived taking into account the residual ICI. The effect of the proposed ICI cancellation scheme is confirmed by computer simulation.

key words: DS-CDMA, frequency-domain equalization, MMSE, ICI cancellation

1. Introduction

The wireless channel is composed of many propagation paths with different time delays, producing frequency-selective multipath fading [1]. Direct-sequence code division multiple access (DS-CDMA) can exploit the channel frequency-selectivity by the use of coherent rake combining that resolves the propagation paths having different time delays and coherently combines them to obtain the path diversity gain [2]. Wideband DS-CDMA [3] has been adopted as a wireless access technique in the 3rd generation (3G) mobile communication systems for data transmissions of up to a few Mbps. Recently, demands for broadband services in mobile communication systems are becoming stronger and stronger and a lot of research attention has been paid to the development of the next generation mobile communication systems that support much higher data rate services than 3G (e.g., higher than a few tens of Mbps) [4]. However, the bit error rate (BER) performance of DS-CDMA with coherent rake combining may significantly degrade due to strong inter-path interference (IPI). Hence, IPI cancellation techniques have been studied for DS-CDMA rake receivers, e.g., [5], [6].

Recently, it has been shown [7]–[11] that frequency-domain equalization (FDE) based on the minimum mean square error (MMSE) criterion can replace the coherent rake

combining while offering much improved BER performance for the DS-CDMA signal reception over a severe frequency-selective channel. In Ref. [7], MMSE-FDE is combined with transmit/receive antenna diversity. MMSE-FDE is applied to multi-code CDMA and the transmission performance with MMSE-FDE is compared with coherent rake combining in Ref. [8]. In Ref. [9], the theoretical BER analysis of DS-CDMA with joint antenna diversity and FDE is presented. The joint use of FDE and multi-access interference (MAI) cancellation for the uplink is considered in Ref. [10] and the downlink CDMA performance with MMSE-FDE is evaluated in Ref. [11].

In this paper, we consider the orthogonal multicode DS-CDMA downlink signal transmission, which requires much higher rate transmission than the uplink as in high speed downlink packet access (HSDPA) [12]. In orthogonal multicode DS-CDMA, as many as SF users (or codes) can be multiplexed, where SF denotes the spreading factor. Although MMSE-FDE improves the BER performance compared to the coherent rake combining, the residual inter-chip interference (ICI) present after MMSE-FDE distorts the orthogonality among the spreading codes and the downlink BER performance degrades as the code multiplexing order increases. In this paper, we propose frequency-domain ICI cancellation to suppress the residual ICI and improve the BER performance of the DS-CDMA downlink signal transmission with MMSE-FDE. In the proposed scheme, the residual ICI replica in the frequency-domain is generated and subtracted from each frequency component of the received signal after MMSE-FDE. The MMSE weight at each iteration is derived taking into account the residual ICI. The effect of the frequency-domain ICI cancellation is evaluated by computer simulation.

The remainder of this paper is organized as follows. Sect. 2 presents a transmission system model. In Sect. 3, frequency-domain ICI replica generation is presented. In Sect. 4, the MMSE weight considering the residual ICI is derived. In Sect. 5, the achievable BER performance in a frequency-selective Rayleigh fading channel is evaluated by computer simulation and the effect of the proposed ICI cancellation is discussed. Section 6 offers some conclusions.

2. Transmission System Model

2.1 Overall Transmission System Model

The transmission system model for DS-CDMA with joint

Manuscript received October 21, 2005.

Manuscript revised May 17, 2006.

[†]The authors are with the Department of Electrical and Communication Engineering, Graduate School of Engineering, Tohoku University, Sendai-shi, 980-8579 Japan.

a) E-mail: takeda@mobile.ecei.tohoku.ac.jp

DOI: 10.1093/ietcom/e89-b.12.3335

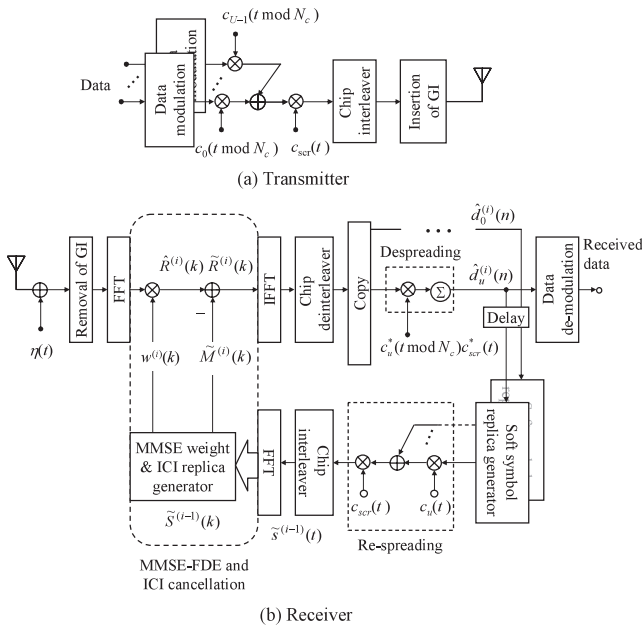


Fig. 1 Transmitter/receiver structure.

MMSE-FDE and ICI canceller is illustrated in Fig. 1. At the base station transmitter, the u th user's binary data sequence, $u = 0 \sim (U - 1)$, is transformed into a data modulated symbol sequence $d_u(n)$ and then spread by multiplying it with an orthogonal spreading sequence $c_u(t)$ of spreading factor SF . The resultant U chip sequences are multiplexed and further multiplied by a common scramble sequence $c_{scr}(t)$ to make the resultant multicode DS-CDMA signal like white-noise. Then, the orthogonal multicode DS-CDMA signal is divided into a sequence of blocks of N_c chips each and then the last N_g chips of each block are copied as a cyclic prefix and inserted into the guard interval (GI) at the beginning of each block.

The GI-inserted orthogonal multicode DS-CDMA signal is transmitted over a frequency-selective fading channel and is received at a receiver. After the removal of the GI, the received chip sequence is decomposed by N_c -point FFT into N_c subcarrier components (the terminology "subcarrier" is used for explanation purpose only although subcarrier modulation is not used). MMSE-FDE is carried out, then, ICI cancellation is performed in the frequency-domain. Inverse FFT (IFFT) is applied to obtain the time-domain received chip sequence for despreading and soft decision. A series of MMSE-FDE, ICI cancellation, IFFT, despreading and soft decision is repeated a sufficient number of times. Finally, data-demodulation is carried out to obtain the received data.

2.2 Transmit and Receive Signals

Throughout this paper, chip-spaced time representation of the transmitted signals is used. Without loss of generality, a transmission of U data symbol sequences $\{d_u(n); n = 0 \sim N_c/SF - 1\}$ is considered, where N_c and SF are chosen so that the value of N_c/SF becomes an integer. The spread signal

chip sequence $\{\hat{s}(t); t = -N_g \sim N_c - 1\}$, to be transmitted after the GI insertion, for one block of $N_c + N_g$ chips can be expressed, using the equivalent lowpass representation, as

$$\hat{s}(t) = \sqrt{2E_c/T_c} s(t \bmod N_c), \quad (1)$$

where E_c and T_c denote the chip energy and the chip duration, respectively, and $s(t)$ is given by

$$s(t) = \left[\sum_{u=0}^{U-1} d_u(\lfloor t/SF \rfloor) c_u(t \bmod SF) \right] c_{scr}(t) \quad (2)$$

with $|c_u(t)| = |c_{scr}(t)| = 1$ for $t = 0 \sim (N_c - 1)$, where $\lfloor x \rfloor$ represents the largest integer smaller than or equal to x .

The propagation channel is assumed to be a frequency-selective block fading channel having chip-spaced L discrete paths, each subjected to independent fading. The assumption of block fading means that the path gains remain constant over at least one block duration. The impulse response $h(t)$ of a multipath channel can be expressed as [13]

$$h(t) = \sum_{l=0}^{L-1} h_l \delta(t - \tau_l), \quad (3)$$

where h_l and τ_l are the complex-valued path gain and time delay of the l th path ($l = 0 \sim L - 1$), respectively, with $\sum_{l=0}^{L-1} E[|h_l|^2] = 1$ ($E[\cdot]$ denotes the ensemble average operation). We assume that the maximum time delay is shorter than the GI length (i.e., $\tau_{L-1} < N_g$). The received chip sequence $\{r(t); t = -N_g \sim N_c - 1\}$ can be expressed as

$$r(t) = \sum_{l=0}^{L-1} h_l \hat{s}(t - \tau_l) + \eta(t), \quad (4)$$

where $\eta(t)$ is a zero-mean complex Gaussian process with a variance of $2N_0/T_c$ with N_0 being the single-sided power spectrum density of the additive white Gaussian noise (AWGN) process.

2.3 MMSE-FDE and ICI Cancellation

A joint MMSE-FDE and ICI cancellation is repeated in an iterative fashion. Below, the i th iteration is described.

After the removal of the GI from the received chip sequence $r(t)$, N_c -point FFT is applied to decompose $\{r(t); t = 0 \sim N_c - 1\}$ into N_c subcarrier components $\{R(k); k = 0 \sim N_c - 1\}$. The k th subcarrier component $R(k)$ can be written as

$$\begin{aligned} R(k) &= \sum_{t=0}^{N_c-1} r(t) \exp\left(-j2\pi k \frac{t}{N_c}\right) \\ &= H(k)S(k) + \Pi(k), \end{aligned} \quad (5)$$

where $S(k)$, $H(k)$ and $\Pi(k)$ are the k th subcarrier component of the transmitted signal sequence $\{s(t); t = 0 \sim N_c - 1\}$ of N_c chips, the channel gain and the noise component due to

the AWGN, respectively. They are given by

$$\begin{cases} S(k) = \sum_{t=0}^{N_c-1} s(t) \exp\left(-j2\pi k \frac{t}{N_c}\right) \\ H(k) = \sqrt{\frac{2E_c}{T_c}} \sum_{l=0}^{L-1} h_l \exp\left(-j2\pi k \frac{\tau_l}{N_c}\right) \\ \Pi(k) = \sum_{t=0}^{N_c-1} \eta(t) \exp\left(-j2\pi k \frac{t}{N_c}\right) \end{cases} \quad (6)$$

MMSE-FDE is carried out as follows:

$$\begin{aligned} \hat{R}^{(i)}(k) &= w^{(i)}(k)R(k) \\ &= S(k)\hat{H}^{(i)}(k) + \hat{\Pi}^{(i)}(k) \end{aligned} \quad (7)$$

with

$$\begin{cases} \hat{H}^{(i)}(k) = w^{(i)}(k)H(k) \\ \hat{\Pi}^{(i)}(k) = w^{(i)}(k)\Pi(k) \end{cases}, \quad (8)$$

where $w^{(i)}(k)$ is the equalization weight at the i th iteration and $\hat{H}^{(i)}(k)$ and $\hat{\Pi}^{(i)}(k)$ are the equivalent channel gain and the noise component, after performing MMSE-FDE at the i th iteration, respectively. The equalization weight is derived in Sect. 4.

The time-domain representation of the signal after MMSE-FDE can be given by

$$\begin{aligned} \hat{r}^{(i)}(t) &= \frac{1}{N_c} \sum_{k=0}^{N_c-1} \hat{R}^{(i)}(k) \exp\left(j2\pi t \frac{k}{N_c}\right) \\ &= A^{(i)}s(t) + \mu^{(i)}(t) + \hat{\eta}^{(i)}(t), \end{aligned} \quad (9)$$

where

$$\begin{cases} A^{(i)} = \frac{1}{N_c} \sum_{k=0}^{N_c-1} \hat{H}^{(i)}(k) \\ \mu^{(i)}(t) = \frac{1}{N_c} \sum_{k=0}^{N_c-1} \hat{H}^{(i)}(k) \left[\sum_{\substack{\tau=0 \\ \tau \neq t}}^{N_c-1} s(\tau) \exp\left(j2\pi k \frac{t-\tau}{N_c}\right) \right] \\ \hat{\eta}^{(i)}(t) = \frac{1}{N_c} \sum_{k=0}^{N_c-1} \hat{\Pi}^{(i)}(k) \exp\left(j2\pi k \frac{t}{N_c}\right) \end{cases} \quad (10)$$

The first term of Eq. (9) is the desired signal, the second is the residual ICI and the third is the noise. The residual ICI $\mu^{(i)}(t)$ after MMSE-FDE distorts the orthogonality among the users. The frequency-domain representation of the residual ICI $\mu^{(i)}(t)$ is given from Eq. (10) by

$$\begin{aligned} M^{(i)}(k) &= \sum_{t=0}^{N_c-1} \mu^{(i)}(t) \exp\left(-j2\pi k \frac{t}{N_c}\right) \\ &= \{\hat{H}^{(i)}(k) - A^{(i)}\} S(k). \end{aligned} \quad (11)$$

ICI cancellation is performed on $\hat{R}^{(i)}(k)$ in the frequency-domain as

$$\tilde{R}^{(i)}(k) = \hat{R}^{(i)}(k) - \tilde{M}^{(i)}(k), \quad (12)$$

where $\tilde{M}^{(i)}(k)$ is the residual ICI replica, given, from Eq. (11), by [14]

$$\tilde{M}^{(i)}(k) = \begin{cases} 0 & \text{for } i = 0 \\ \{\hat{H}^{(i)}(k) - A^{(i)}\} \tilde{S}^{(i-1)}(k) & \text{for } i > 0 \end{cases}, \quad (13)$$

where $\tilde{S}^{(i-1)}(k)$ is the k th frequency component of the transmitted chip replica, which is generated by feeding back the $(i-1)$ th ICI cancellation result. After the residual ICI cancellation, N_c -point IFFT is applied to transform the frequency-domain signal $\{\tilde{R}^{(i)}(k); k = 0 \sim N_c - 1\}$ into time-domain chip sequence $\{\tilde{r}^{(i)}(t); t = 0 \sim N_c - 1\}$ and then despreading is carried out on $\tilde{r}^{(i)}(t)$ to obtain the decision variable for $d_u(n)$ as

$$\hat{d}_u^{(i)}(n) = \frac{1}{SF} \sum_{t=nSF}^{(n+1)SF-1} \tilde{r}^{(i)}(t) c_u^*(t \bmod SF) c_{scr}^*(t), \quad (14)$$

which is the soft decision variable associated with $d_u(n)$ after the i th iteration.

3. ICI Replica Generation

In this section, we consider the $i(\geq 1)$ th iteration. ICI replica generation for the i th iteration is presented.

The soft decision variable is used to generate the replica $\{\tilde{s}^{(i-1)}(t); t = 0 \sim N_c - 1\}$ of the transmitted chip sequence so as to avoid the error propagation due to the erroneous decision variable.

Using the soft decision variable $\hat{d}_u^{(i-1)}(n)$ associated with $d_u(n)$, the log-likelihood ratio (LLR) for the x th bit in the n th symbol $d_u(n)$ ($n = 0 \sim N_c/SF - 1$), where $x = 0 \sim \log_2 K - 1$ and K is the modulation level, can be computed as [15]

$$\begin{aligned} L_x^{(i-1)}(n) &= \ln \left(\frac{p^{(i-1)}(b_{n,x} = 1)}{p^{(i-1)}(b_{n,x} = 0)} \right) \\ &\approx \frac{\left| \hat{d}_u^{(i-1)}(n) - A^{(i-1)} a_{b_{n,x}=0}^{\min} \right|^2}{2\hat{\sigma}^2} \\ &\quad - \frac{\left| \hat{d}_u^{(i-1)}(n) - A^{(i-1)} a_{b_{n,x}=1}^{\min} \right|^2}{2\hat{\sigma}^2} \end{aligned} \quad (15)$$

where $p^{(i-1)}(b_{n,x} = 1)$ and $p^{(i-1)}(b_{n,x} = 0)$ are the probabilities of the transmitted bit $b_{n,x}$ being $b_{n,x} = 1$ and $b_{n,x} = 0$, respectively, when expected at the $(i-1)$ th iteration. $a_{b_{n,x}=0}^{\min}$ (or $a_{b_{n,x}=1}^{\min}$) is the most probable symbol that gives the minimum Euclidean distance from $\hat{d}_u^{(i-1)}(n)$ among all candidate symbols with $b_{n,x} = 0$ (or 1). $2\hat{\sigma}^2$ is the variance of the noise plus residual ICI and is given by Appendix A

$$2\hat{\sigma}^2 = \frac{1}{SF} \left[\frac{2N_0}{T_c} \frac{1}{N_c} \sum_{k=0}^{N_c-1} |w^{(i-1)}(k)|^2 + \left(\frac{\rho^{(i-2)}}{N_c} \right) \left\{ \frac{1}{N_c} \sum_{k=0}^{N_c-1} |\hat{H}^{(i-1)}(k)|^2 - |A^{(i-1)}|^2 \right\} \right], \quad (16)$$

where $\rho^{(i)}$ will be derived in Sect. 4.

The soft decision symbol $\tilde{d}_u^{(i-1)}(n)$, $n = 0 \sim N_c/SF - 1$, can be obtained using [16]

$$\tilde{d}_u^{(i-1)}(n) = \sum_{d \in D} d \prod_{b_{n,x} \in d} p^{(i-1)}(b_{n,x}), \quad (17)$$

where d represents the candidate symbol having $b_{n,x} = 0$ or $b_{n,x} = 1$ in the symbol set D and $p^{(i-1)}(b_{n,x} = 0)$ and $p^{(i-1)}(b_{n,x} = 1)$ are given, from Eq. (15), by

$$\begin{cases} p^{(i-1)}(b_{n,x} = 0) = -\frac{1}{2} \tanh\left(\frac{L_x^{(i-1)}(n)}{2}\right) + \frac{1}{2} \\ p^{(i-1)}(b_{n,x} = 1) = \frac{1}{2} \tanh\left(\frac{L_x^{(i-1)}(n)}{2}\right) + \frac{1}{2} \end{cases} \quad (18)$$

since $p^{(i-1)}(b_{n,x} = 1) + p^{(i-1)}(b_{n,x} = 0) = 1$.

$\tilde{d}_u^{(i-1)}(n)$ of Eq. (17) is the expectation of the transmitted symbol, and it is used as a soft decision symbol replica as in [16]. For QPSK data modulation and 16-quadrature amplitude modulation (16QAM), $\tilde{d}_u^{(i-1)}(n)$ becomes (see Appendix B)

$$\begin{cases} \tilde{d}_u^{(i-1)}(n) = \frac{1}{\sqrt{2}} \tanh\left(\frac{L_0^{(i-1)}(n)}{2}\right) + j \frac{1}{\sqrt{2}} \tanh\left(\frac{L_1^{(i-1)}(n)}{2}\right) \\ \text{for QPSK} \\ \tilde{d}_u^{(i-1)}(n) = \frac{1}{\sqrt{10}} \tanh\left(\frac{L_0^{(i-1)}(n)}{2}\right) \left\{ 2 + \tanh\left(\frac{L_1^{(i-1)}(n)}{2}\right) \right\} \\ + j \frac{1}{\sqrt{10}} \tanh\left(\frac{L_2^{(i-1)}(n)}{2}\right) \left\{ 2 + \tanh\left(\frac{L_3^{(i-1)}(n)}{2}\right) \right\} \\ \text{for 16QAM} \end{cases} \quad (19)$$

The replica $\{\tilde{s}^{(i-1)}(t); t = 0 \sim N_c - 1\}$ of the transmitted chip sequence $s(t)$ is generated as

$$\tilde{s}^{(i-1)}(t) = \left[\sum_{u=0}^{U-1} \tilde{d}_u^{(i-1)}(\lfloor t/SF \rfloor) c_u(t \bmod SF) \right] c_{scr}(t). \quad (20)$$

Then, N_c -point FFT is applied to decompose the replica $\tilde{s}^{(i-1)}(t)$ into N_c subcarrier components $\{\tilde{S}^{(i-1)}(k); k = 0 \sim (N_c - 1)\}$ as

$$\tilde{S}^{(i-1)}(k) = \sum_{t=0}^{N_c-1} \tilde{s}^{(i-1)}(t) \exp\left(-j2\pi k \frac{t}{N_c}\right). \quad (21)$$

Substituting Eq. (21) into Eq. (13), we obtain the frequency-domain ICI replica $M^{(i)}(k)$.

4. MMSE Weight Derivation

At the first iteration ($i = 0$), MMSE-FDE is performed before the ICI cancellation and therefore, the MMSE weight given in [8], [9] is used. However, the residual ICI is suppressed after ICI cancellation and therefore, the MMSE

weight needs to be updated in each iteration ($i > 0$). In this paper, the MMSE weight, taking into account the residual ICI $M^{(i)}(k)$, is derived at each iteration. To derive the MMSE weight, we define the equalization error $e(k)$ between the frequency component $\{\tilde{R}^{(i)}(k); k = 0 \sim N_c - 1\}$ after the ICI cancellation and the transmitted frequency component $\{S(k); k = 0 \sim N_c - 1\}$ as

$$\begin{aligned} e(k) &= \tilde{R}^{(i)}(k) - A^{(i)}S(k) \\ &= \left\{ w^{(i)}(k)H(k) - A^{(i)} \right\} \left\{ S(k) - \tilde{S}^{(i-1)}(k) \right\} + w^{(i)}(k)\Pi(k), \end{aligned} \quad (22)$$

where $A^{(i)}S(k)$ is used as a reference signal since $E[\tilde{R}^{(i)}(k)] = A^{(i)}S(k)$ (the residual ICI is assumed to have zero-mean value). $w^{(i)}(k)$ is the weight that minimizes the MSE $E[|e(k)|^2]$ for the given $H(k)$, i.e., $\partial E[|e(k)|^2]/\partial w^{(i)}(k) = 0$.

Since $\Pi(k)$ is a zero-mean complex Gaussian process with variance $2\sigma^2 (= 2N_0N_c/T_c)$, $E[|e(k)|^2]$ is given by

$$E[|e(k)|^2] = \rho^{(i-1)} \left| w^{(i)}(k)H(k) - A^{(i)} \right|^2 + 2\sigma^2 \left| w^{(i)}(k) \right|^2, \quad (23)$$

where

$$\begin{aligned} \rho^{(i-1)} &= E \left[\left| S(k) - \tilde{S}^{(i-1)}(k) \right|^2 \right] \\ &= E \left[\left| \sum_{t=0}^{N_c-1} \left\{ s(t) - \tilde{s}^{(i-1)}(t) \right\} \exp\left(-j2\pi k \frac{t}{N_c}\right) \right|^2 \right] \\ &= \sum_{t=0}^{N_c-1} E \left[\left| s(t) - \tilde{s}^{(i-1)}(t) \right|^2 \right]. \end{aligned} \quad (24)$$

$\tilde{s}^{(i-1)}(t)$ is obtained by spreading $\tilde{d}_u^{(i-1)}(n)$ as in Eq. (20), where $\tilde{d}_u^{(i-1)}(n)$ is the expectation of $d_u(n)$ at the $(i-1)$ th iteration (i.e., $\tilde{d}_u^{(i-1)}(n) = E[d_u(n)]$) as shown in Eq. (17). Since $\tilde{s}^{(i-1)}(t)$ is the expectation of $s(t)$ at the $(i-1)$ th iteration (i.e., $\tilde{s}^{(i-1)}(t) = E[s(t)]$ at the $(i-1)$ th iteration), Eq. (24) can be rewritten as

$$\rho^{(i-1)} = \sum_{t=0}^{N_c-1} \left\{ E \left[|s(t)|^2 \right] - |\tilde{s}^{(i-1)}(t)|^2 \right\}. \quad (25)$$

In Eq. (25), $s(t)$ is unknown. Therefore, we remove the expectation operation from $E[|s(t)|^2]$ and replace $s(t)$ by the hard decision chip sequence replica $\bar{s}^{(i-1)}(t)$. Replacing $s(t)$ in Eq. (25) by $\bar{s}^{(i-1)}(t)$, we have

$$\rho^{(i-1)} \approx \sum_{t=0}^{N_c-1} \left\{ \left| \bar{s}^{(i-1)}(t) \right|^2 - |\tilde{s}^{(i-1)}(t)|^2 \right\}. \quad (26)$$

$\bar{s}^{(i-1)}(t)$ is generated as follows. The tentative data decision is performed on $\tilde{d}_u^{(i-1)}(n)$ of Eq. (14) to obtain the hard decision symbol replica $\tilde{d}_u^{(i-1)}(n)$. Then, re-spreading and re-scrambling are applied to $\tilde{d}_u^{(i-1)}(n)$ to obtain

$$\bar{s}^{(i-1)}(t) = \left[\sum_{u=0}^{U-1} \tilde{d}_u^{(i-1)}(\lfloor t/SF \rfloor) c_u(t \bmod SF) \right] c_{scr}(t). \quad (27)$$

The following MMSE weight is obtained (see Appendix C):

$$w^{(i)}(k) = \frac{H^*(k)}{\rho^{(i-1)} |H(k)|^2 + 2\sigma^2} \quad (28)$$

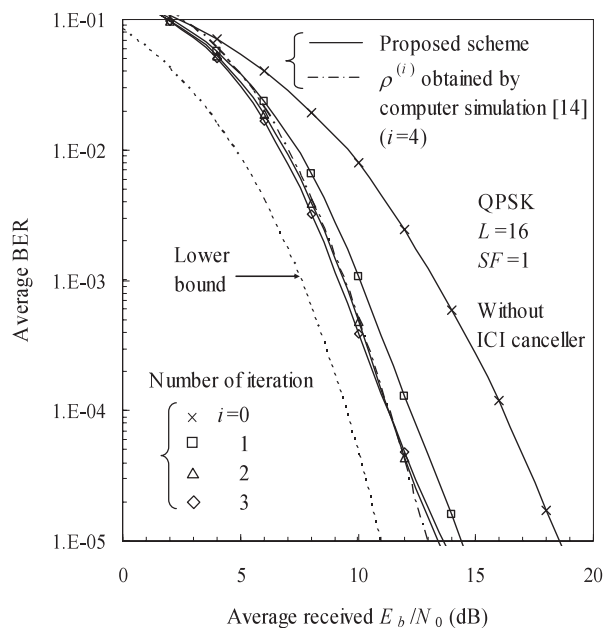
where $\rho^{(-1)} = 1$.

5. Computer Simulation

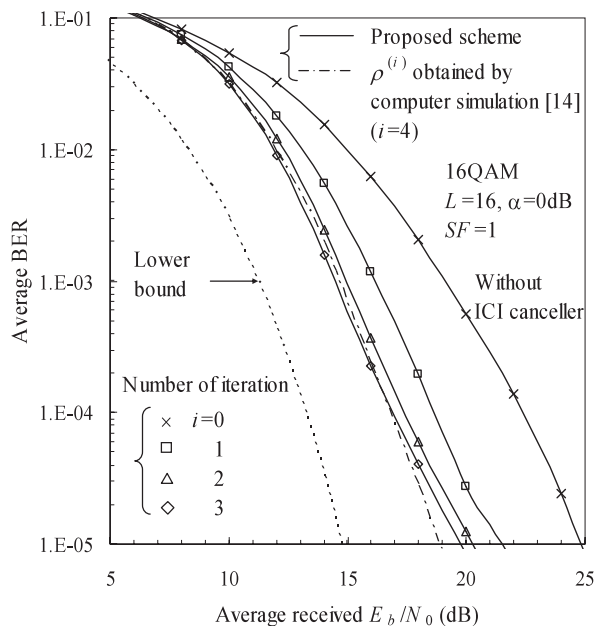
The simulation parameters are summarized in Table 1. We assume QPSK data modulation and 16QAM, an FFT block size of $N_c = 256$ chips and a GI of $N_g = 32$ chips. The channel is assumed to be a frequency-selective block Rayleigh fading channel having a chip-spaced L -path uniform power delay profile (i.e., $E[|h_l|^2] = 1/L$ for all l). Perfect chip timing and ideal channel estimation are assumed.

The simulated BER performance of frequency-domain ICI cancellation is plotted in Fig. 2 for $SF = U = 1$ as a function of the average received bit energy-to-AWGN noise power spectrum density ratio E_b/N_0 , defined as $E_b/N_0 = (1/\log_2 K)SF(E_c/N_0)(1 + N_g/N_c)$. For comparison, the theoretical lowerbound [9] and the BER performance of $i = 4$ using $\rho^{(i)}$ optimized by computer simulation at each iteration [14] are also plotted. In [14], the computer-optimized $\rho^{(i)}$ were found by computer simulation as $\rho^{(0)} = 1, \rho^{(1)} = 0.2, \rho^{(2)} = 0.1, \rho^{(3)} = 0.05$ and $\rho^{(4)} = 0$ for QPSK and $\rho^{(0)} = 1, \rho^{(1)} = 0.15, \rho^{(2)} = 0.1, \rho^{(3)} = 0.05$ and $\rho^{(4)} = 0.05$ for 16QAM. The BER performance with $i = 0$ corresponds to the case of MMSE-FDE without ICI cancellation. It can be seen from Fig. 2 that the proposed ICI cancellation can significantly improve the BER performance and achieve almost the same BER performance as the ICI cancellation using the computer-optimized $\rho^{(i)}$. When $i = 1$ and 3, the E_b/N_0 reduction for BER = 10^{-4} from the case without ICI cancellation is as much as 4 and 4.9 dB, respectively, for QPSK and the BER performance of $i = 3$ gets close to the theoretical lowerbound by about 1.9 dB (including a 0.5 dB loss due to the GI insertion). There may be two reasons for this performance gap of 1.9 dB. (1) The computer-optimized $\rho^{(i)}$ is

optimum only in the average sense; it is optimized by taking into account all the channel conditions. Hence, $\rho^{(i)}$ is not necessarily optimum for a certain fading channel condition. (2) As can be seen from Eq. (9), $A^{(i)}$ of the desired signal $A^{(i)}s(t)$ after MMSE-FDE is equivalent to the channel gain of a frequency-non selective channel. Since $A^{(i)}$ is the average of N_c different equivalent channel gains, the probability that $A^{(i)}$ drops (or fades) is very low. However, once $A^{(i)}$ drops, many symbols in a block are likely to be detected in error; this degrades the accuracy of the symbol replica generation and hence the ICI cancellation can not perform



(a) QPSK

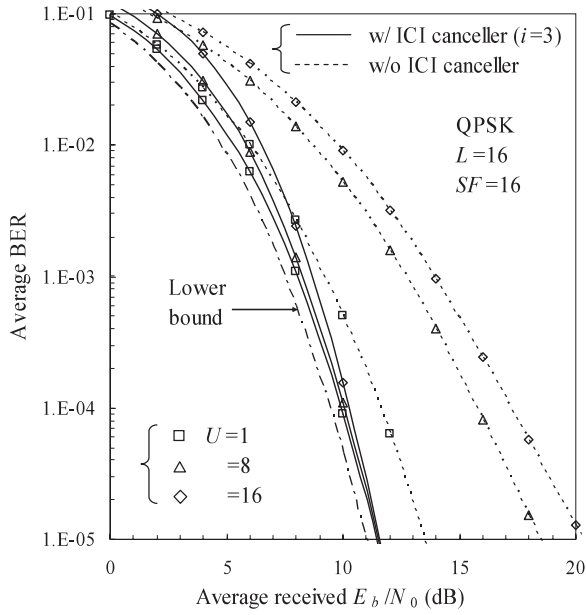


(b) 16QAM

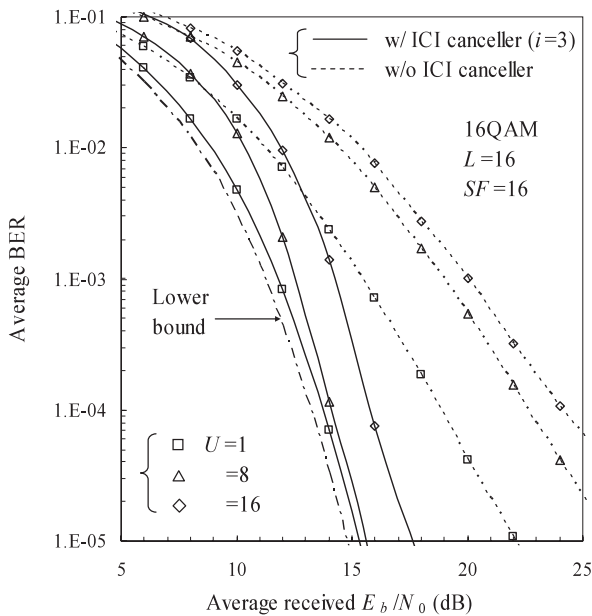
Table 1 Simulation parameters.

Transmitter	Modulation	QPSK, 16QAM
	Number of FFT points	$N_c=256$
	GI	$N_g=32(\text{chip})$
	Spreading sequence	Product of Walsh sequence and PN sequence
	Spreading factor	$SF=1\sim 64$
Channel	Fading	Frequency-selective block Rayleigh fading
	Power delay profile	$L=16$ -path uniform power delay profile
Receiver	Channel estimation	Ideal

Fig. 2 BER performance with frequency-domain ICI cancellation with MMSE-FDE for $SF = U = 1$.



(a) QPSK



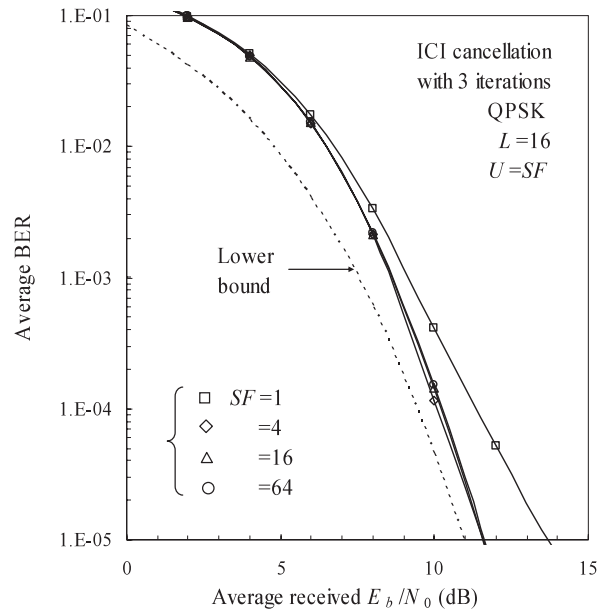
(b) 16QAM

Fig. 3 BER performance with frequency-domain ICI cancellation with MMSE-FDE for $SF = 16$.

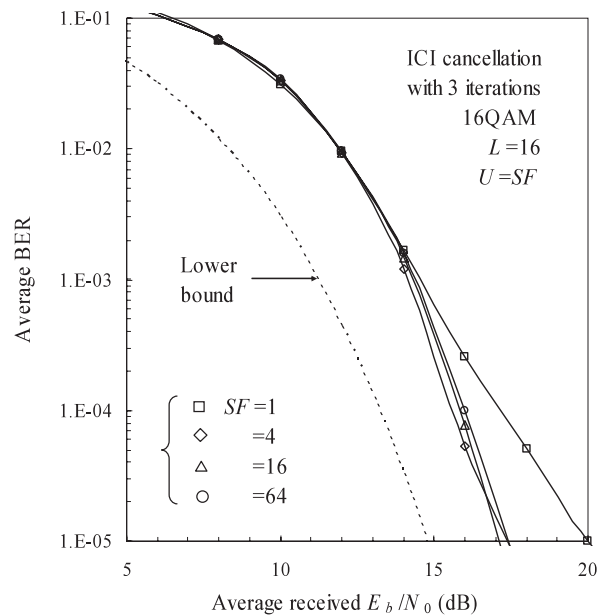
satisfactorily.

For 16QAM (see Fig. 2(b)), the Euclidean distance between different symbols is shorter and hence, decision error due to the residual ICI is more likely than for QPSK. ICI cancellation is found to be very effective to improve the BER performance even for 16QAM. An E_b/N_0 reduction of as much as 5.4 dB can be achieved for $BER = 10^{-4}$.

The BER performance for the case of $SF = 16$ is plotted in Fig. 3 with U as a parameter. When $U = 1$, the BER performance is better for $SF = 16$ than for $SF = 1$ (compare Figs. 2 and 3) since the residual ICI can be better suppressed by the despreading process. When $U = 1$, both for



(a) QPSK



(b) 16QAM

Fig. 4 BER performance of multicode transmission for the same data rate.

QPSK and 16QAM, the BER performance approaches the theoretical lowerbound by about 0.5 dB. As U increases, the BER performance degrades for the no ICI cancellation case. This is because a severe orthogonality distortion is caused by the residual ICI. The use of ICI cancellation can improve the BER performance. When $U = 16$, the E_b/N_0 reduction from the no ICI cancellation case is as much as 6.9 (8.3) dB for QPSK (16QAM).

The BER performance of multicode DS-CDMA with frequency-domain ICI cancellation of 3 iterations is plotted for the same data rate (i.e., for the same U/SF) in Fig. 4 with SF as a parameter for $SF = U$. Almost the same BER per-

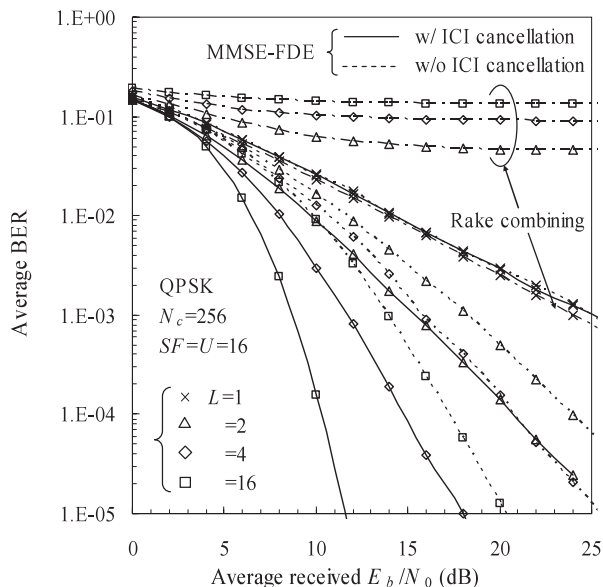


Fig. 5 Effect of channel frequency-selectivity.

formance is obtained when $SF \geq 4$ and is better than the $SF = 1$ case (non spread transmission). The reason for this is that the residual ICI after the ICI cancellation can be suppressed by the despreading process for $SF \geq 4$, however, this is not the case when $SF = 1$. When $SF \geq 4$, an E_b/N_0 reduction of about 1 dB from the $SF = 1$ case is observed for both QPSK and 16QAM. However, note that the multicode DS-CDMA signal has larger peak-to-average power ratio (PAPR) although it gives better BER performance than SC transmission (i.e., $SF = 1$).

The extent to which the BER performance is improved depends on the channel frequency-selectivity (the channel frequency-selectivity gets stronger as the number L of paths increases). The simulated BER performance using ICI cancellation is plotted in Fig. 5 with L as a parameter for QPSK data modulation and $SF = U = 16$. For comparison, the BER performances without ICI cancellation and using rake combining are also plotted. With MMSE-FDE, as L increases, the BER performance improves since larger frequency diversity gain can be obtained. However, with rake combining, the BER performance gets worse as L increases. This is because of severer orthogonality distortion among the codes due to larger ICI. When $L = 1$, the BER performance is the same as without ICI cancellation since the ICI is not present (the performance degradation of 0.5 dB from rake combining is owing to the loss due to the GI insertion). When $L \geq 2$, ICI cancellation can significantly improve the BER performance. Even when $L = 2$, an E_b/N_0 reduction of 3 dB is achieved for $BER = 10^{-4}$.

6. Conclusion

In this paper, we proposed a joint frequency-domain ICI cancellation and MMSE-FDE. The MMSE weight taking into account the residual ICI was derived. The BER perfor-

mance with the proposed ICI cancellation was evaluated by computer simulation. It was found that, when $SF = U = 16$, the E_b/N_0 reduction for achieving $BER = 10^{-4}$ from the no cancellation case is as much as about 6.9 (8.3) dB for QPSK (16QAM). The performance comparison between the multicode DS-CDMA and the non spread signal transmission have shown that multicode DS-CDMA (i.e., $SF \geq 4$) provides better BER performance than the non spread signal transmission. In this paper, we assumed ideal channel estimation and have shown how close the proposed ICI cancellation brings a BER performance to the theoretical lower-bound. The impact of the channel estimation error on the ICI cancellation is left for a future work.

References

- [1] F. Adachi, "Wireless past and future—Evolving mobile communications systems," *IEICE Trans. Fundamentals*, vol.E84-A, no.1, pp.55–60, Jan. 2001.
- [2] W.C. Jakes, Jr., ed., *Microwave Mobile Communications*, Wiley, New York, 1974.
- [3] F. Adachi, M. Sawahashi, and H. Suda, "Wideband DS-CDMA for next generation mobile communications systems," *IEEE Commun. Mag.*, vol.36, no.9, pp.56–69, Sept. 1998.
- [4] Y. Kim et al., "Beyond 3G: Vision, requirements, and enabling technologies," *IEEE Commun. Mag.*, vol.41, no.3, pp.120–124, March 2003.
- [5] K. Higuchi, K. Okawa, M. Sawahashi, and F. Adachi, "Field experiments on pilot symbol-assisted coherent multistage interference canceller in DS-CDMA reverse link," *IEICE Trans. Commun.*, vol.E86-B, no.1, pp.191–205, Jan. 2003.
- [6] S. Moshavi, "Multi-user detection for DS-CDMA communications," *IEEE Commun. Mag.*, vol.34, no.10, pp.124–136, Oct. 1996.
- [7] F.W. Vook, T.A. Thomas, and K.L. Baum, "Cyclic-prefix CDMA with antenna diversity," *Proc. IEEE VTC 2002 Spring*, pp.1002–1006, May 2002.
- [8] F. Adachi, T. Sao, and T. Itagaki, "Performance of multicode DS-CDMA using frequency domain equalization in a frequency selective fading channel," *Electron. Lett.*, vol.39, pp.239–241, Jan. 2003.
- [9] F. Adachi and K. Takeda, "Bit error rate analysis of DS-CDMA with joint frequency-domain equalization and antenna diversity combining," *IEICE Trans. Commun.*, vol.E87-B, no.10, pp.2991–3002, Oct. 2004.
- [10] S. Tomasin and N. Benvenuto, "Equalization and multiuser interference cancellation in CDMA systems," *Proc. 6th International Symposium on Wireless Personal Multimedia Communication (WPMC)*, vol.1, pp.10–14, Yokosuka, Japan, Oct. 2003.
- [11] I. Martoyo, G.M.A. Sessler, J. Luber, and F.K. Jondral, "Comparing equalizers and multiuser detections for DS-CDMA downlink systems," *Proc. IEEE VTC 2004-Spring*, pp.1649–1653, May 2004.
- [12] Physical layer aspects of UTRA High Speed Downlink Packet Access (Release 4), March 2001. 3GPP, 3G TR25.848 V4.0.0.
- [13] T.S. Rappaport, *Wireless Communications*, Prentice Hall, 1996.
- [14] K. Takeda and F. Adachi, "Iterative frequency-domain inter-chip interference cancellation for DS-CDMA," *Proc. 8th WPMC*, Aalborg, Denmark, Sept. 2005.
- [15] A. Stefanov and T. Duman, "Turbo coded modulation for wireless communications with antenna diversity," *Proc. IEEE VTC99-Fall*, pp.1565–1569, Netherlands, Sept. 1999.
- [16] X. Wang and H.V. Poor, "Iterative (turbo) soft interference cancellation and decoding for coded CDMA," *IEEE Trans. Commun.*, vol.47, no.7, pp.1046–1061, July 1999.

Appendix A: Derivation of $\hat{\sigma}^2$

The residual ICI $\bar{\mu}(n)$ and the noise component $\bar{\eta}(n)$ after the despreading of the i th iteration are given by

$$\begin{aligned}\bar{\mu}(n) &= \frac{1}{SF} \sum_{t=nSF}^{(n+1)SF-1} c^*(t) \\ &\times \frac{1}{N_c} \sum_{k=0}^{N_c-1} \left\{ \hat{H}^{(i)}(k) - A^{(i)} \right\} \left\{ S(k) - \tilde{S}^{(i-1)}(k) \right\} \exp\left(j2\pi k \frac{t}{N_c}\right) \\ \bar{\eta}(n) &= \frac{1}{SF} \frac{1}{N_c} \sum_{t=nSF}^{(n+1)SF-1} c^*(t) \sum_{k=0}^{N_c-1} \hat{\Pi}(k) \exp\left(j2\pi k \frac{t}{N_c}\right).\end{aligned}\quad (\text{A}\cdot 1)$$

Since the spreading sequence $c(t)$ is like white-noise, $E[c(t)c^*(\tau)] = \delta(t - \tau)$, and hence, the variance of $\bar{\mu}(n)$ is given by

$$\begin{aligned}\sigma_{ICI}^2 &= \frac{1}{2} \frac{1}{SF^2} \frac{1}{N_c^2} \sum_{t=nSF}^{(n+1)SF-1} \sum_{k=0}^{N_c-1} \sum_{k'=0}^{N_c-1} \\ &E \left[\left\{ \hat{H}^{(i)}(k) - A^{(i)} \right\} \left\{ S(k) - \tilde{S}^{(i-1)}(k) \right\} \right. \\ &\left. \times \left\{ \hat{H}^{(i)*}(k') - A^{(i)*} \right\} \left\{ S^*(k') - \tilde{S}^{(i-1)*}(k') \right\} \right] \\ &\times \exp\left(j2\pi(k - k') \frac{t}{N_c}\right),\end{aligned}\quad (\text{A}\cdot 2)$$

The residual ICI component $\left\{ \hat{H}^{(i)}(k) - A^{(i)} \right\} \left\{ S(k) - \tilde{S}^{(i-1)}(k) \right\}$ at the k th frequency is assumed to be a zero-mean random variable. Hence, we have

$$\sigma_{ICI}^2 = \frac{1}{2} \frac{1}{SF} \frac{1}{N_c^2} \sum_{k=0}^{N_c-1} \left| \hat{H}^{(i)}(k) - A^{(i)} \right|^2 E \left[\left| S(k) - \tilde{S}^{(i-1)}(k) \right|^2 \right].\quad (\text{A}\cdot 3)$$

Since $\rho^{(i-1)} = E \left[\left| S(k) - \tilde{S}^{(i-1)}(k) \right|^2 \right]$ from the definition in Eq. (24),

$$\sigma_{ICI}^2 = \frac{1}{2} \frac{1}{SF} \frac{1}{N_c} \rho^{(i-1)} \left[\frac{1}{N_c} \sum_{k=0}^{N_c-1} \left| \hat{H}^{(i)}(k) \right|^2 + \left| A^{(i)} \right|^2 \right] \left[-2 \operatorname{Re} \left[\frac{1}{N_c} \sum_{k=0}^{N_c-1} \hat{H}^{(i)}(k) A^{(i)} \right] \right].\quad (\text{A}\cdot 4)$$

Since $A^{(i)} = \frac{1}{N_c} \sum_{k=0}^{N_c-1} \hat{H}^{(i)}(k)$, we obtain

$$\sigma_{ICI}^2 = \frac{1}{2} \frac{1}{SF} \frac{1}{N_c} \rho^{(i-1)} \left[\frac{1}{N_c} \sum_{k=0}^{N_c-1} \left| \hat{H}^{(i)}(k) \right|^2 - \left| A^{(i)} \right|^2 \right].\quad (\text{A}\cdot 5)$$

Next, the variance of $\bar{\eta}(n)$ is given by

$$\begin{aligned}\sigma_{noise}^2 &= \frac{1}{SF^2} \frac{1}{N_c^2} \sum_{t=nSF}^{(n+1)SF-1} \sum_{k=0}^{N_c-1} \sum_{k'=0}^{N_c-1} E \left[\hat{\Pi}(k) \hat{\Pi}^*(k') \right] \\ &\times \exp\left(j2\pi(k - k') \frac{t}{N_c}\right).\end{aligned}\quad (\text{A}\cdot 6)$$

Since $\Pi(k)$ is a zero-mean complex Gaussian process with variance $2\sigma^2 = 2N_0N_c/T_c$, $\hat{\Pi}(k)$ is also a zero-mean variable, and hence, we have

$$\sigma_{noise}^2 = \frac{1}{SF} \frac{N_0}{T_c} \left(\frac{1}{N_c} \sum_{k=0}^{N_c-1} \left| w^{(i)}(k) \right|^2 \right).\quad (\text{A}\cdot 7)$$

From Eqs. (A-5) and (A-7), $2\hat{\sigma}^2$ is given by

$$2\hat{\sigma}^2 = 2\hat{\sigma}_{ICI}^2 + 2\hat{\sigma}_{noise}^2.\quad (\text{A}\cdot 8)$$

Appendix B: Soft Decision Symbol Replica $\tilde{d}_u^{(i-1)}(n)$

For QPSK, Eq. (17) is written as

$$\begin{aligned}\tilde{d}_u^{(i-1)}(n) &= \left(\frac{1}{\sqrt{2}} + j \frac{1}{\sqrt{2}} \right) p(b_{n,0} = 1) p(b_{n,1} = 1) \\ &+ \left(-\frac{1}{\sqrt{2}} + j \frac{1}{\sqrt{2}} \right) p(b_{n,0} = 0) p(b_{n,1} = 1) \\ &+ \left(-\frac{1}{\sqrt{2}} - j \frac{1}{\sqrt{2}} \right) p(b_{n,0} = 0) p(b_{n,1} = 0) \\ &+ \left(\frac{1}{\sqrt{2}} - j \frac{1}{\sqrt{2}} \right) p(b_{n,0} = 1) p(b_{n,1} = 0).\end{aligned}\quad (\text{A}\cdot 9)$$

Substituting Eq. (18) into Eq. (A-9) gives

$$\tilde{d}_u^{(i-1)}(n) = \frac{1}{\sqrt{2}} \tanh\left(\frac{L_0(n)}{2}\right) + j \frac{1}{\sqrt{2}} \tanh\left(\frac{L_1(n)}{2}\right).\quad (\text{A}\cdot 10)$$

For 16QAM, Eq. (17) is written as

$$\begin{aligned}\tilde{d}_u^{(i-1)}(n) &= \left(\frac{3}{\sqrt{10}} + j \frac{3}{\sqrt{10}} \right) p(b_{n,0} = 1) p(b_{n,1} = 1) p(b_{n,2} = 1) p(b_{n,3} = 1) \\ &+ \left(\frac{3}{\sqrt{10}} + j \frac{1}{\sqrt{10}} \right) p(b_{n,0} = 1) p(b_{n,1} = 1) p(b_{n,2} = 1) p(b_{n,3} = 0) \\ &+ \left(\frac{3}{\sqrt{10}} - j \frac{1}{\sqrt{10}} \right) p(b_{n,0} = 1) p(b_{n,1} = 1) p(b_{n,2} = 0) p(b_{n,3} = 0) \\ &+ \left(\frac{3}{\sqrt{10}} - j \frac{3}{\sqrt{10}} \right) p(b_{n,0} = 1) p(b_{n,1} = 1) p(b_{n,2} = 0) p(b_{n,3} = 1) \\ &+ \dots\end{aligned}\quad (\text{A}\cdot 11)$$

Substituting of Eq. (18) into Eq. (A-11) gives

$$\begin{aligned}\tilde{d}_u^{(i-1)}(n) &= \frac{1}{\sqrt{10}} \tanh\left(\frac{L_0(n)}{2}\right) \left\{ 2 + \tanh\left(\frac{L_1(n)}{2}\right) \right\} \\ &+ j \frac{1}{\sqrt{10}} \tanh\left(\frac{L_2(n)}{2}\right) \left\{ 2 + \tanh\left(\frac{L_3(n)}{2}\right) \right\}.\end{aligned}\quad (\text{A}\cdot 12)$$

Appendix C: Derivation of MMSE Weight

Let $w^{(i)}(k)$, $H(k)$ and $A^{(i)}$ be

$$\begin{cases} w^{(i)}(k) = x_k + jy_k \\ H(k) = u_k + jv_k \\ A^{(i)} = a + jb \end{cases} \quad (\text{A} \cdot 13)$$

Using Eq. (A-13), Eq. (23) can be rewritten as

$$\begin{aligned} E[|e(k)|^2] &= \rho^{(i-1)} (x_k u_k - y_k v_k - a)^2 \\ &\quad + \rho^{(i-1)} (x_k v_k + y_k u_k - b)^2 \\ &\quad + 2\sigma^2 (x_k^2 + y_k^2). \end{aligned} \quad (\text{A} \cdot 14)$$

$w^{(i)}(k)$ is the weight that minimizes the mean square error $E[|e(k)|^2]$ for the given $H(k)$, i.e.,

$$\frac{\partial E[|e(k)|^2]}{\partial w^{(i)}(k)} = \frac{\partial E[|e(k)|^2]}{\partial x_k} + j \frac{\partial E[|e(k)|^2]}{\partial y_k} = 0. \quad (\text{A} \cdot 15)$$

$\partial E[|e(k)|^2]/\partial x_k$ and $\partial E[|e(k)|^2]/\partial y_k$ are respectively given by

$$\begin{cases} \frac{\partial E[|e(k)|^2]}{\partial x_k} = 2\rho^{(i-1)} u_k (x_k u_k - y_k v_k - a) \\ \quad + 2\rho^{(i-1)} v_k (x_k v_k + y_k u_k - b) + 4\sigma^2 x_k \\ \frac{\partial E[|e(k)|^2]}{\partial y_k} = -2\rho^{(i-1)} v_k (x_k u_k - y_k v_k - a) \\ \quad + 2\rho^{(i-1)} u_k (x_k v_k + y_k u_k - b) + 4\sigma^2 y_k \end{cases} \quad (\text{A} \cdot 16)$$

Hence, we have

$$\begin{aligned} \frac{\partial E[|e(k)|^2]}{\partial w^{(i)}(k)} &= \frac{\partial E[|e(k)|^2]}{\partial x_k} + j \frac{\partial E[|e(k)|^2]}{\partial y_k} \\ &= 2\rho^{(i-1)} w^{(i)}(k) |H(k)|^2 - 2\rho^{(i-1)} A^{(i)} H^*(k) \\ &\quad + 4\sigma^2 w^{(i)}(k). \end{aligned} \quad (\text{A} \cdot 17)$$

From $\partial E[|e(k)|^2]/\partial w^{(i)}(k) = 0$, we have

$$w^{(i)}(k) = \frac{H^*(k)}{\rho^{(i-1)} |H(k)|^2 + 2\sigma^2}. \quad (\text{A} \cdot 18)$$



Kazuaki Takeda received his B.E. and M.S. degree in communications engineering from Tohoku University, Sendai, Japan, in 2003 and 2004, respectively. Currently he is a PhD student at the Department of Electrical and Communications Engineering, Graduate School of Engineering, Tohoku University. His research interests include equalization, interference cancellation, transmit/receive diversity, and multiple access techniques. He was a recipient of the 2003 IEICE RCS (Radio Communication Systems) Active Research Award and 2004 Inose Scientific Encouragement Prize.



Koichi Ishihara received his B.S. and M.S. degrees in communications engineering from Tohoku University, Sendai, Japan, in 2004 and 2006, respectively. Since April 2006, he has been with NTT Network Innovation Laboratories, Nippon Telegraph & Telephone Corporation (NTT), Yokosuka, Japan. His research interests include equalization, interference cancellation, and multiple access techniques for broadband wireless communication systems.



Fumiuyuki Adachi received the B.S. and Dr. Eng. degrees in electrical engineering from Tohoku University, Sendai, Japan, in 1973 and 1984, respectively. In April 1973, he joined the Electrical Communications Laboratories of Nippon Telegraph & Telephone Corporation (now NTT) and conducted various types of research related to digital cellular mobile communications. From July 1992 to December 1999, he was with NTT Mobile Communications Network, Inc. (now NTT DoCoMo, Inc.), where he led a research group on wideband/broadband CDMA wireless access for IMT-2000 and beyond. Since January 2000, he has been with Tohoku University, Sendai, Japan, where he is a Professor of Electrical and Communication Engineering at the Graduate School of Engineering. His research interests are in CDMA wireless access techniques, equalization, transmit/receive antenna diversity, MIMO, adaptive transmission, and channel coding, with particular application to broadband wireless communications systems. From October 1984 to September 1985, he was a United Kingdom SERC Visiting Research Fellow in the Department of Electrical Engineering and Electronics at Liverpool University. Dr. Adachi served as a Guest Editor of IEEE JSAC on Broadband Wireless Techniques, October 1999, Wideband CDMA I, August 2000, Wideband CDMA II, Jan. 2001, and Next Generation CDMA Technologies, Jan. 2006. He is an IEEE Fellow and was a co-recipient of the IEEE Vehicular Technology Transactions Best Paper of the Year Award 1980 and again 1990 and also a recipient of Avant Garde award 2000. He was a recipient of IEICE Achievement Award 2002 and a co-recipient of the IEICE Transactions Best Paper of the Year Award 1996 and again 1998. He was a recipient of Thomson Scientific Research Front Award 2004.